Role of TGF-β in a Mouse Model of High Turnover Renal Osteodystrophy†

Shiguang Liu[1], **Wenping Song**[1], **Joseph H Boulanger**[1], **Wen Tang**[1], **Yves Sabbagh**[1], **Brian Kelley**[1], **Russell Gotschall**[1], **Susan Ryan**[1], **Lucy Phillips**[1], **Katie Malley**[1], **Xiaohong Cao**[1], **Tai-He Xia**[1], **Gehua Zhen**[2], **Xu Cao**[2], **Hong Ling**[1], **Paul C Dechow**[3], **Teresita M Bellido**[4], **Steven R Ledbetter**[1], and **Susan C Schiavi**[1]

[1]Genzyme, a Sanofi Company, Sanofi-Genzyme R& D Center, Framingham, MA, USA

[2]Department of Orthopedic Surgery, Johns Hopkins Medical Institution, Baltimore, MD, USA

[3]Department of Biomedical Sciences, Baylor College of Dentistry, Texas A&M Health Science Center, Dallas, TX, USA

[4]Department of Anatomy and Cell Biology, Division of Endocrinology, and Department of Medicine, Indiana University School of Medicine, Indianapolis, IN, USA

Abstract

Altered bone turnover is a key pathologic feature of chronic kidney disease-mineral and bone disorder (CKD-MBD). Expression of TGF-β1, a known regulator of bone turnover, is increased in bone biopsies from individuals with CKD. Similarly, TGF-β1 mRNA and downstream signaling is increased in bones from *jck* mice, a model of high-turnover renal osteodystropy. A neutralizing anti-TGF-β antibody (1D11) was used to explore TGF-βs role in renal osteodystrophy. 1D11 administration to *jck* significantly attenuated elevated serum osteocalcin and type I collagen C-telopeptides. Histomorphometric analysis indicated that 1D11 administration increased bone volume and suppressed the elevated bone turnover in a dose-dependent manner. These effects were associated with reductions in osteoblast and osteoclast surface areas. μCT confirmed the observed increase in trabecular bone volume and demonstrated improvements in trabecular architecture and increased cortical thickness. 1D11 administration was associated with significant reductions in expression of osteoblast marker genes (Runx2, alkaline phosphatase, osteocalcin) and the osteoclast marker gene, Trap5. Importantly, in this model, 1D11 did not improve kidney

---

*Address correspondence to: Shiguang Liu, MD, PhD, Genzyme Science Center, Sanofi, 49 New York Ave., Framingham, MA 01701. USA. shiguang.liu@genzyme.com.

function or reduce serum PTH levels indicating that 1D11 effects on bone are independent of changes in renal or parathyroid function. 1D11 also significantly attenuated high turnover bone disease in the adenine-induced uremic rat model. Antibody administration was associated with a reduction in pSMAD2/SMAD2 in bone but not bone marrow as assessed by quantitative immunoblot analysis. Immunostaining revealed pSMAD staining in osteoblasts and osteocytes but not osteoclasts, suggesting 1D11 effects on osteoclasts may be indirect. Immunoblot and whole genome mRNA expression analysis confirmed our previous observation that repression of Wnt/β catenin expression in bone is correlated with increased osteoclast activity in *jck* mice and bone biopsies from CKD patients. Furthermore, our data suggests that elevated TGF-β may contribute to the pathogenesis of high turnover disease partially through inhibition of β-catenin signaling.

Keywords

Growth Factors; HORMONES and RECEPTORS; Wnt/Frz/LRP5; PARACRINE SIGNALING; Rodent; ANIMAL MODELS; Bone histomorphometry; QUANTITATION; Bone turnover markers; QUANTITATION

Introduction

Skeletal complications associated with renal failure have been well documented in individuals with chronic kidney disease (CKD) from stage 3 through dialysis. (1–5) Furthermore, evidence is accumulating to suggest that at least some individuals with stage 2 CKD also have poor bone health. (5–8) These findings are relevant given that poor bone health and cardiovascular disease appear inter-related and cardiovascular events are the major cause of mortality in CKD patients. (9–11) Importantly, agents that enhance bone quality also reduce cardiovascular disease. (12–15) In late stages of the disease, elevated PTH and serum phosphorus (Pi) can be mechanistically linked to bone and cardiovascular disease through well characterized mechanisms. (16) As anticipated, treatments that lower PTH and/or serum phosphorus provide positive benefits on bone and cardiovascular health. (3,17–22) Nonetheless, as elevations in PTH and Pi are rather late events in CKD progression, these pathologies may not be sufficient to explain the growing evidence for declining bone and cardiovascular health occurring prior to their elevation. An understanding of the pathologic mechanisms associated with these early skeletal and vascular changes may lead to the generation of transformative therapies.

Given the challenges of performing longitudinal studies based on clinical bone biopsies, we and others have begun to assess early bone changes in genetic rodent models that develop progressive CKD. (4,6,23) We recently described molecular and phenotypic bone changes throughout the development of renal osteodystrophy in the CKD model, *jck* mice. *Jck* mice develop polycystic kidney disease as a result of a mutation in NEK8, a protein responsible for trafficking of two cilia-associated proteins, polycystin 1 and 2. (24,25) Despite a clear role for cilia in normal bone remodeling (26,27), we have previously demonstrated that the underlying defect in *jck* mice is insufficient to directly influence bone health in the absence of reduced renal function.(6) Our data also showed that early repression of osteocyte Wnt/β-catenin signaling was associated with increased osteoclast activity which was independent of

detectable PTH changes. Furthermore, we also demonstrated that osteocyte Wnt/β-catenin signaling is altered in bone biopsies from individuals with CKD, underscoring the relevance of this newly characterized model of renal osteodystrophy. Finally, we showed that biphasic changes in Wnt/β-catenin antagonist expression also occur both in *jck* mouse and clinical bone biopsies.(6) This evidence is supported by clinical epidemiologic studies demonstrating increased serum levels of sclerostin, an antagonist of the Wnt/β-catenin pathway in CKD and dialysis patients. (28,29)

The factors responsible for early changes in sclerostin and β-catenin signaling have not yet been identified but one viable candidate is TGF-β1, the most abundant bone cytokine. (30) Under physiological conditions, TGF-β1 is a major modulator of bone turnover that plays diverse roles throughout the remodeling cycle. It regulates bone remodeling by recruiting mesenchymal stem cells to bone remodeling sites, enhancing differentiation of bone marrow mesenchymal stem cells, enhancing osteoblast precursor proliferation, and inhibiting osteoblast differentiation. (31–36) Pharmacologic inhibition of TGF-beta receptor signaling in osteoblasts increases bone mass by reducing the rate of remodeling, providing additional evidence for TGFβ's role in bone health. (37) Furthermore, TGFβ antagonism via a neutralizing antibody leads to significant enhancement of bone quality in normal mice. (38)

TGF-β1 protein is elevated in bone biopsies from individuals with end stage renal disease where it is thought to contribute to increased fibrosis associated with cortical bone porosity. (39,40) Given the important role of this factor in bone biology, it is conceivable that high bone levels of TGF-β in CKD may contribute to renal osteodystrophy (ROD). The availability of a neutralizing PAN – anti TGF-β antibody provided the means to directly explore the potential role of this cytokine in the development of renal osteodystrophy in both *jck* mice and adenine induced rat models of CKD. (6,25,41) Our data demonstrates that TGF-β signaling is significantly increased in osteoblasts and early osteocytes and 1D11 attenuates high-turnover disease, at least in part through specific effects on osteoblast lineage cells by promoting enhanced β-catenin signaling. These data support a role of TGF-β in the pathogenesis of high turnover renal osteodystrophy.

Methods

In vivo evaluation of 1D11 effects on bone

Wild-type (WT) (C57BL/6J) and *jck* mice were originally obtained from Jackson labs (Bar Harbor, Maine, USA). Eight to nine week old male NTac:SD rat were purchased from Taconic and Yecuris Corporation (Germantown, NY, USA). All animals for the studies were maintained in a virus- and parasite-free barrier facility with a 12-h light/dark cycle. All animal procedures were conducted in accordance with approved Institutional Animal Care and Use Committee (IACUC) protocols. Unless otherwise specified, both mice and rats were maintained on standard rodent chow diet (PicoLab Rodent Diet 20, LabDiet, St. Louis, MO, USA) containing 0.63% phosphate, 0.81% calcium with 2.2 IU/gram Vitamin D_3.

At 5 wks of age, *jck* mice were switched to a casein-based diet containing 0.4% calcium and 1.0% phosphate (Diet # D08112306; Research Diets Inc., New Brunswick, NJ, USA) to induce hyperphosphatemia. To explore the role of TGF-β on the progression of renal

osteodystrophy, the neutralizing anti-TGF-β antibody, 1D11 (Genzyme, a Sanofi Company) or vehicle was given to *jck* mice at 8–9 weeks of age via intraperitoneal injection 3 times per week at 0, 2 or 5 mg/kg. Because a potential mechanism of 1D11 was unknown at the initiation of these studies, we designed two studies that spanned the different mechanistic phases. As bone turnover in mouse is about 3 weeks, we designed studies that spanned one or two bone remodeling periods and chose 4 and 7 week treatment periods to evaluate 1D11 effects on bone histomorphometric parameters. Blood and tissues were collected after 4 or 7 weeks of treatment (n = 15 for the 4 week treatment study and n = 12 for the 7 week treatment study). In contrast to histomorphometric changes, primary effects on gene expression and signaling occur more rapidly. To evaluate 1D11's influence on mechanisms associated with bone turnover we utilized bone samples from 12 week old mice given 4 injections at 5 mg/kg for a week. Bones were collected 7 days after the first injection for gene expression and immunoblot analysis, as described in the results and figure legends.

To induce uremia in rats, 10 week old male NTac:SD rats were fed standard rodent diet containing 0.6% adenine for 1 week, followed by a diet containing 0.3% adenine for 5 weeks, and then standard rodent diet without adenine for the remaining 4 weeks of the study. The evaluation of 1D11 effect's in the rat adenine model included 3 groups (n = 8 per group): (1) normal control: rats on the standard diet; (2) adenine group: adenine + vehicle (PBS); (3) 1D11 group: adenine + 1D11. 1D11 or vehicle was administered to the adenine treated rats from the beginning of the study via intraperitoneal injection 3 times per week at 10 mg/kg for 10 weeks. Serum and tissue samples were collected after 10 weeks of treatment.

Blood and urine biochemistry

Whole blood was collected under isofluorane anesthesia via retro-orbital bleed, incubated for 20 minutes at room temperature, and then centrifuged at 4°C. Serum was aliquoted and frozen at −80°C for subsequent analysis. Serum phosphate (Pi), calcium (Ca), blood urea nitrogen (BUN) and creatinine (enzymatic method) were measured on an Integra 400 bioanalyzer (Roche Diagnostics, Indianapolis, IN, USA). Intact PTH (Immutopics, San Clemente, CA, USA), 1, 25-dihydroxyvitamin D ($1,25(OH)_2D_3$) (IDS, Fountain Hills, AZ, USA), serum osteocalcin (OCN) (Biomedical Technologies Inc, Stoughton, MA, USA), serum c-telopeptide of type I collagen (CTX) (IDS, Fountain Hills, AZ, USA), N-terminal propeptide of type I procollagen (P1NP) (IDS, Fountain Hills, AZ, USA); intact FGF23 (Kainos, Tokyo, Japan) ELISAs; Mouse/Rat SOST Immunoassay Quantikine ELISA (R&D systems) were performed according to manufacturer's instructions.

Tissue harvest and histology

Tissues were harvested, fixed in 10% Neutral Buffered Formalin (NBF) for 24–48 hours, and then placed in 70% ethanol. Processed tissues were paraffin embedded and sectioned. Sections were dewaxed in xylene, rehydrated by ethanol gradient and stained in hematoxylin and eosin. For bone immunostaining, femurs were decalcified, processed and embedded in paraffin and sectioned. For dynamic bone histomorphometric analysis, mice were given intraperitoneal injections of Alizarin complexone (ACROS, Fair Lawn, NJ, USA) 7 days before sacrifice (40 mg/kg) and calcein (15 mg/kg) 2 days before sacrifice. Femurs were

fixed in 40% alcohol, processed and embedded in methyl methacrylate. Each femur was sectioned in the ventral/dorsal plane. Two levels per block separated by 100 microns were selected for staining. Goldner's Trichrome and von Kossa sections were analyzed for static measurements. Unstained serial sections were used for dynamic measurements using the Osteo II Bioquant system (BIOQUANT, Nashville, TN, USA). Nomenclature is in agreement with recommendations by Parfitt *et al.* (42)

Cortical bone resorption score were evaluated based on number and size of the resorption canals. The samples were evaluated blind by a certified veterinary pathologist. The scoring system was defined as follows: 0: No significant lesions; 1: a few scattered small resorption canals; 2: more frequent, small-medium sized resorption canals; 3: more prominent cortical resorption canals, beginning to coalesce; 4: numerous large coalescing cortical resorption canals, sometimes extending full thickness through the cortex.

Immunohistochemistry and TRAP staining of mouse bones

Five-micrometer paraffin de-waxed and rehydrated sections were used. TRAP staining was performed using standard protocol (Sigma-Aldrich). The number of TRAP positive osteoclasts in femurs was counted using the Osteo II Bioquant system. The region of interest (ROI) was defined by tracing an area from the growth plate to 500 microns below with exclusion of cortical bone. The number of TRAP positive osteoclasts was normalized to bone surface.

Immunostaining was also performed using a standard protocol. Briefly, the sections were incubated with Trypsin Retrieval Solution (BioGenex, Fremont, CA, USA) at 37°C for 20 min followed by PBS washes. The sections were then treated with 0.3% H_2O_2 in methanol for 30 minutes and blocked with 2.5% normal horse serum. Slides were incubated overnight at 4°C in blocking buffer containing the primary antibody, goat anti-pSMAD2/3 (1:100) (Santa Cruz Biotechnology Inc., USA). After washing in PBST, the slides were incubated in ImmPRESS Reagent anti-goat IgG (Vector Laboratories, Burlingame, CA, USA), washed in PBST, developed with diaminobenzidine substrate (Vector Laboratories, Burlingame, CA, USA), and counterstained with Mayer's hematoxylin. The slides were then washed in tap water for 5 minutes, dehydrated, cleared, and mounted with Cytoseal XYL (Thermo, Rockford, IL. USA). Images were visualized on a Zeiss Axiovert 200.

TUNEL staining

Osteocyte apoptosis was detected by TdT-mediated dUTP nick-end labeling (TUNEL) using a modified version of a commercial kit (Calbiochem, Gibbstown, NJ) in longitudinal sections of the femur counterstained with 2% methyl green, as previously described. (43,44) Osteocyte apoptosis and empty lacunae were separately assessed in the cancellous and cortical bone of the distal metaphysis. The metaphysis was defined as the area starting 0.5 mm from the most proximal part of the growth plate and extending 0.5 mm towards the diaphysis.

Micro-computed tomography (μCT) analysis of bone

Tibias were imaged by μCT using isotopic voxels at a resolution of 3.5 microns (AG Micro-CT 35, Scanco Medical, Brüttisellen, Switzerland). Fifty slices of mid-diaphyseal cortical bone (175 microns total thickness) were analyzed with a threshold of 565 mg/cc. The following variables were calculated using Scanco software routines and compared between groups: bone volume fraction (BV/TV), apparent density (density of cortical bone including resorption spaces and voids) (data not shown) and material density (BMD) (threshold set for cortical bone density only). The nomenclature, symbols, and units used correspond to those described by Bouxsein *et al*.(45)

Strength testing

Tibias were tested by 3-point bending, and the strength parameter (maximum load at failure) was assessed with a Test Resources (Shakopee, MN, USA) DDL200 axial loading machine outfitted with an Interface SMT1-22 force transducer. Cross-head displacement rate was 0.1 mm/sec. Tests were conducted on the mid-diaphyses with the bones resting on two supports 5mm apart and the tibial anterior margins facing upward toward the actuator.

Colony formation unit (CFU) assay and osteoclastogenesis in vitro

Bone marrow was collected from 12 week old female WT or *jck* animals treated with PBS or 1D11 at 2 or 5 mg/kg, 3 times a week for 2 weeks and cultured in αMEM containing 15% heat inactivated fetal bovine serum (HI-FBS), and penicillin-streptomycin (Invitrogen, Carlsbad, CA, USA). Media was replaced 3 days post adherence and refreshed 7 days thereafter. After 13 days, adherent cells were plated at 5000 cells/cm^2 in triplicate in six well plates and cultured in differentiation media, αMEM, 50 μg/ml ascorbic acid, 10% HI-FBS, penicillin-streptomycin. Media was replaced every 4 days. At day 8, cells were fixed and stained for alkaline phosphatase activity with 10 mg naphthol AS-MX, 20 mg Fast Blue BB salt, 1 ml N,N-dimethylformaide, in 19 ml of 0.1 M Tris (pH 9.2) (all from Sigma, St. Louis, MO, USA) to detect CFU-osteoblast (CFU-OB). Colonies greater than 1 mm in diameter were counted. CFU-fibroblasts (CFU-F) were detected by staining the same plates with 0.2% crystal violet in 2% ethanol for 1 hour. Plates were washed with water and then air-dried. All colonies greater than 1 mm in diameter were counted to yield the percentage of CFU-OB/CFU-F. To induce differentiation of HSCs to osteoclasts, bone marrow cells were cultured in αMEM containing 10% HI-FBS, 5 ng/ml macrophage colony-stimulating factor (M-CSF) (Sigma, St. Louis, MO, USA) and penicillin-streptomycin (Invitrogen, Carlsbad, CA, USA). 48 hours later, the non-adherent cells were collected, counted and plated in 96-well plates at a density of 1.5×10^5 cells/well in αMEM containing 10% HI-FBS, 60 ng/ml M-CSF, 50 ng/ml Receptor activator of nuclear factor kappa-B ligand (RANKL) and penicillin-streptomycin for 9 days. Cells were then stained for TRAP staining kit (Sigma, St. Louis, MO, USA). TRAP positive cells with 3 or more nuclei were considered osteoclasts and counted.

Gene expression analysis

Bone shafts were collected, epiphysis removed, bone marrow displaced via centrifugation, and the shafts placed in Trizol (Sigma, St. Louis, MO, USA). RNA was extracted using the

Trizol, chloroform and isopropanol precipitation method. The extracted RNA was treated with DNase, purified on a Qiagen (Valencia, CA, USA) column and eluted in RNAse free water. A reverse transcriptase reaction was performed. The generated cDNA was used in single Taqman assays or customized Taqman low density arrays (TLDA) (Applied Biosystems, Carlsbad, CA, USA) containing genes of interest.

For whole genome mRNA expression analysis, 7 and 11 week *jck* mice received injections of PBS or 1D11 (5 mg/kg) at days 1, 3, 5 and 7. Long bones were collected from these animals at day 8 (8 or 12 weeks old) and age-matched WT mice to serve as controls. Six animals were used in each group. Total RNA was isolated from bone shafts using TRizol (Invitrogen). RNA sequencing libraries were constructed using Illumina (San Diego, CA) mRNA sequencing kits by BGI America. Libraries were subsequently sequenced on Illumina Hiseq2000 sequencer by BGI to a depth of 30 million total reads (paired end & 90 bps read length). Fastq files containing clean sequence reads (PCR primer & adapter sequences removed) were then loaded into ArrayStudio (OmicSoft, NC) for QC and analysis. Low quality reads were removed and then aligned against mouse genome B37 and gene model Ensembl R65. Total read counts were summarized using the gene model and RPKM (reads per kilobase per million reads) values were generated for each gene. Differential gene expression fold differences and p values were then generated by ANOVA analysis. Significantly expressed gene list (fold cut off 1.2 and p value < 0.05) were then loaded into IPA (Ingenuity, CA) pathway analysis software for downstream functional analysis.

Immunoblot analysis

Bone marrow and bone shafts from tibia and femur were frozen in liquid nitrogen, pulverized and protein was extracted with 50 mM Tris buffer (pH 7.4), containing 0.1 M sodium chloride and 0.1% Triton X-100. Bone marrow or bone extracts were denatured at 70°C for 10 minutes and then separated by electrophoresis on 8% Bis-Tris gels (Invitrogen). Separated proteins were electrotransferred to nitrocellulose (NC) membranes followed by incubation in blocking buffer (5% nonfat dry milk in Tris buffered saline, pH 7.4, and 0.3% Tween 20). Membranes were then incubated overnight at 4°C in blocking buffer containing one of the following primary antibodies: rabbit polyclonal antiserum pSMAD2 (Cell Signaling Technology, Inc.) (1:500), rabbit polyclonal anti-β-catenin (phospho S37) antibody (Abcam) (1:500) or mouse monoclonal primary antiserum SMAD2 (1:1000) was incubated with membrane overnight at 4 °C in blocking buffer. The membrane was washed 5 times with TBS contained 0.1% Tween 20 (TBST) for 10 minutes each wash. For detection of pSMAD2 or p-β-catenin, the secondary antibody incubation was performed for 60 minutes at room temperature using anti-rabbit IgG conjugated to horseradish peroxidase (Cell Signaling Technology, Inc.) at dilution of 1:5000. The secondary anti-mouse IgG conjugated to horseradish peroxidase (Cell Signaling Technology, Inc.) at dilution of 1:5000 was used as secondary antibody for SMAD2 detection. After final washing, the immunoreactive bands were detected using an enhanced chemiluminescence reagent (SuperSignal West Dura, Thermo Scientific), read on film, and quantitated using Image J software. Antiserum to β-Actin (Abcam) was incubated room temperature for 1 hour at 1:50,000 dilution, washed, and quantified as well and used as a loading control.

Statistical analysis

All values are reported as the mean ± standard error of the mean (SEM) and were analyzed by one-way ANOVA or *t*-test using GraphPad Prism version 5.00 for Windows (GraphPad Software, San Diego California USA).

Results

TGF-β1 expression and signaling are increased in bone of *jck* mice, a high turnover model of CKD-MBD

The *jck* mouse is a genetic model of polycystic kidney disease (PKD) that has a progressive decline in renal function. (25) We have recently demonstrated that these mice also exhibit prominent features of CKD-MBD including altered serum chemistries, high-turnover ROD and cardiovascular disease. (6) In addition to the previously reported increases in BUN and serum PTH, an increased number of surface TRAP positive osteoclasts was observed in femur sections that is consistent with high bone turnover (Fig. 1).

As a first step in exploring whether TGF-β contributes to the pathogenesis of high-turnover ROD, we first measured mRNA expression of the major isoform, TGF-β1 and its receptor, TGFβR1 in bone. TGF-β1 mRNA expression was significantly increased by about 1.7 fold in *jck* by 9 weeks of age (data not shown) and sustained throughout disease progression (Fig. 2A). TGFβR1 mRNA expression was also elevated in bones of *jck* compared with WT mice at both 12 and 16 weeks of age (Fig. 2*A*). However neither the cytokine nor its receptor was significantly elevated in bone marrow (Fig. 2*B*). Immunoblot analysis confirmed that increased expression of TGF-β1 and TGFβR1 was associated with activation of SMAD signaling based on increased expression of pSMAD2 and total SMAD2 protein in bone but not bone marrow (Fig. 2*C*). The ratio of pSMAD2 and SMAD proteins (pSMAD/SMAD) measured by quantitative immunoblot analysis was also increased in bone but not bone marrow (Fig. 2*C*). To further identify the specific cell types within bone that respond to TGF-β1, pSMAD2/3 immunostaining was performed on decalcified bone sections. pSMAD2/3 staining appeared more intense in osteoblasts and early osteocytes in *jck* bone. In addition, osteoblasts in *jck* were more cuboidal relative to those observed in WT-derived bones (Fig. 2*D*). Importantly, pSMAD2/3 expression did not co-localize with TRAP positive osteoclasts (Fig. 2*E*).

The neutralizing anti-TGF-β antibody (1D11) attenuated the increased bone turnover in *jck* mice

1D11, a neutralizing anti-TGF-β antibody was administered to *jck* mice starting at 8 weeks of age for 4 or 7 weeks (Fig. 3). We have previously shown that 8 wk old *jck* mice have evidence of early stages of high turnover disease. (6) To determine the effect of anti-TGF-β antibody on turnover, serum biomarkers were measured. 1D11 (5mg/kg) resulted in a trend toward reduced OCN but not CTX at 4 weeks and significantly attenuated the elevation of both serum bone turnover markers after 7 weeks of treatment (Fig. 4*A, B*). A significant suppression of CTX and a trend toward suppression of serum OCN after 7 weeks of treatment were observed at 2 mg/kg. Consistent with its effects on serum OCN, 1D11 at 5 mg/kg also attenuated the elevation of serum P1NP levels in the 7-week treatment study

(Table 1). 1D11 had no effect on either serum BUN or PTH levels indicating that 1D11 did not significantly affect kidney function or PTH production/secretion in this study (Fig. 4*C, D*). Similarly, 1D11 did not influence the known alterations in serum Pi, Ca, 1,25(OH)$_2$D$_3$ or FGF23 levels (Table 1).

Dynamic and static bone histomorphometric analysis was performed on non-decalcified femur sections and reported using the TMV (turnover, mineralization and bone volume) classification recommended by KDIGO (Fig. 5*A*–*C*) along with the full analysis (Table 2) (1). Consistent with the observed changes in serum bone turnover biomarkers, 1D11 dose-dependently suppressed bone turnover measured by bone formation rates at 12 weeks of age after 7 weeks of treatment (Fig. 5*A*). Despite suppression of bone turnover, bone volume was significantly increased without impacting bone mineralization lag time in each treatment group (2 and 5 mg/kg) (Fig. 5*B, C*; Table 2). Evaluation of the decalcified bone sections with H&E and TRAP staining, showed a trend toward improvement in cortical bone resorption in *jck* mice by 1D11 treatment (5 mg/kg) (Fig. 5*D, E*).

In agreement with findings from histomorphometric analysis, μCT analysis on femurs after 4 weeks of treatment (5 mg/kg 1D11) also demonstrated increased fractional bone volume (BV/TV) and trabecular number (Tb.N), with a corresponding decrease in trabecular separation (Tb.Sp) (Fig. 6). 1D11 administration was also associated with increased bone mineral density (both apparent and material density) and cortical thickness (Fig. 6). Finally, 1D11 administration was associated with an increased trend in bone strength as determined by 3-point bending test. The yield strengths were measured at 14.4 ± 1.1 N and 15.2 ± 0.7 N in *jck* treated with PBS and 1D11 (5 mg/kg), respectively.

1D11 suppresses osteoblast and osteoclast function in *jck* mice

We have previously demonstrated that in addition to increased bone formation rates, *jck* bones have increased osteoblast and osteoclast numbers. 1D11 suppressed both osteoblast and osteoclast numbers on trabecular bone surfaces at 5 mg/kg after 4 and 7 weeks of treatment (Fig. 7*A*). Gene expression analysis by RT-PCR (7-week treatment) confirmed that 1D11 administration was associated with significant reductions in mRNA for markers of osteoblast differentiation including osteocalcin (Bglap), osterix (Sp7), runx2, and alkaline phosphatase (Alpl) and the osteoclast marker, Trap5 (Fig. 7*B*). Additionally, trends toward reduced expression of the osteoclast genes, cathepsin K (Ctsk) and Tnfrsf11a (Rank) were also observed.

Normal coupling between osteoclast and osteoblast activities at the sites of remodeling was demonstrated by co-localization of TRAP staining with immunostaining for the osteoblast marker, osterix (Fig. 7*C*). Both TRAP and anti-osterix staining were significantly suppressed by 1D11, further demonstrating that inhibition of TGF-β reduced both osteoblastogenesis and osteoclastogenesis (Fig. 7*C*). These data indicated that 1D11 inhibited bone turnover without significantly disrupting the coupling between bone resorption and formation.

1D11 attenuates high turnover bone disease in rat adenine induced-CKD model

To confirm that the role of TGF-β in *jck* mice represents a general phenomenon in ROD and is not specific to the *jck* mouse model, we evaluated 1D11's influence on bone in a moderate rat adenine-induced CKD model in which animals were fed diets that had declining doses of adenine as described in the Methods section. Adenine treatment resulted in renal damage as demonstrated by increased serum BUN levels. Importantly, similar to our findings in the *jck* mouse model, 1D11 treatment had no significant effect on renal function (Fig. 8*A*). Consistent with observations in *jck* mice, serum bone turnover markers, OCN and CTX, were significantly elevated in the adenine treated group and were both significantly attenuated by 1D11 treatment (Fig. 8*B, C*). Bone histomorphometric analysis confirmed an increase in both osteoblast and osteoclast surface areas consistent with increased bone turnover that were attenuated with 1D11 treatment (Fig. 8E, F). Similar to findings in *jck* mice, 1D11 treatment was also associated with a strong trend toward improved bone volume (p=0.06) (Fig. 8D).

1D11 reduces SMAD2 signaling in bone

To explore the mechanism by which 1D11 influences osteoblast and osteoclast number and/or function, we first examined 1D11 induced early changes in the canonical TGF-β signaling pathway, SMAD2/3. Eleven week old *jck* mice received 4 doses of 1D11 (5 mg/kg) prior to sacrifice over a course of one week (Fig. 3). Quantitative immunoblot analysis of protein extracted from the mid-shaft of both tibia and femur confirmed the initial observation that the pSMAD2/SMAD2 ratio was increased in *jck* mice and demonstrated that a one week treatment with 1D11 significantly attenuated the increase (Fig. 9*A.B*).

As described above, changes in pSMAD2/SMAD2 were not observed via immunoblot of whole bone marrow. To explore the possibility that 1D11 may influence the subset of osteoprogenitor cells, we assessed the influence of antibody treatment on the differentiation potential of bone marrow mesenchymal (MSC) and hematopoetic stem cells (HSC). 1D11 (5 mg/kg) was administered to *jck* starting at 10 weeks of age (Fig 3). After 2 weeks of treatment (12 weeks of age), bone marrow was collected from age matched WT, treated and untreated *jck* and cultured under conditions that favored either MSC differentiation to osteoblasts or HSC differentiation to osteoclasts. CFU-OB/CFU-F ratio was significantly increased from *jck* mice compared to WT mice. 1D11 at 5 mg/kg significantly suppressed the CFU-OB/CFU-F ratio in *jck* mice (Fig. 10 *A*), whereas, the number of osteoclast progenitors was similar between WT and *jck* mice. 1D11 treatment had no influence on the osteoclastic differentiation potential (Fig. 10*B*).

We also determined whether the higher number of osteoclasts observed in bones of *jck* mice were a consequence of increased osteoclast recruitment by apoptotic osteocytes, and if so whether 1D11 could attenuate these changes (Fig. 10 *C*). However, our data did not support this hypothesis as the number of TUNEL positive osteocytes was significantly decreased in *jck* compared to age-matched WT mice. Furthermore, no differences were observed between 1D11 treated versus untreated *jck* mice.

1D11 treatment restores β-catenin pathway changes

We have previously shown that an underlying decrease in β-catenin signaling is associated with ROD in *jck* bones and human bone biopsies. (6). Immunoblot analysis confirmed the increased expression of the inactive form of β-catenin (p-β-catenin) in protein isolated from *jck* femurs in comparison to WT bones at 12 weeks of age. Importantly, one week of 1D11 administration was associated with a decrease in p-β-catenin protein to a level similar to that observed in WT mice (Fig. 3 and 10 *D*). Modulation of Wnt/β-catenin pathway components and downstream gene expression changes were further explored using whole genome RNA sequence analysis on bone samples from the 1-week study at 12 weeks of age (Fig. 3). As shown in Table 3, expression of genes whose products are within or downstream of the canonical Wnt/β-catenin pathway are consistent with an overall repression of this pathway in *jck* mice relative to WT mice. Genes that were significantly down-regulated included ligands (Wnt16, Wnt10B and Wnt5B) and receptors/co-receptors (Frzb and Lrp5) of this pathway. β-catenin (Ctnnb1), the most important downstream component of the Wnt pathway was also significantly suppressed. Within those genes that were up-regulated in expression, sFrp1, sFrp4 and Dkkl1 are all negative regulators of Wnt signaling. In addition, consistent with previously described gene expression data from RT-PCR, Tgf-β1 and Tgfbr1 were significantly elevated. Furthermore, after one week of 1D11 administration, many genes within the Wnt/β-catenin pathway were regulated toward normal levels (Table 4). Among the genes up-regulated by 1D11, the most important gene in the Wnt pathway, β-catenin (Ctnnb1) was completely normalized. In addition, Wnt receptors (Fzd5 and Smo), downstream elements (Dvl1 and Dvl3) and the positive regulator (Appl2) were up-regulated after 1 week of 1D11 treatment. β-casein kinase 2 was the only down-regulated gene in the pathway, which was up-regulated in *jck* and completely normalized by 1D11. Importantly, β-catenin target genes such as Pkd1 were normalized by 1D11.

Expression of Sost, a Wnt antagonist, was decreased in *jck* bones compared to WT mice at 12 weeks of age most likely due to significantly elevated serum PTH levels (Table 3, Fig 11 *A* and Fig. 1). 1D11 treatment was associated with a strong trend toward a further suppression of Sost mRNA expression in the *jck* bones at this time point. As we have previously shown, Sost mRNA expression is most highly up-regulated at an earlier CKD stage in this model and in human bone biopsies and may contribute to the early repression of osteocyte Wnt/βcatenin signaling. Therefore to understand the effect of 1D11 on Sost expression, we performed a similar 1 week 1D11 study using 7 week old mice (Fig. 3). Consistent with our previous observation, Sost mRNA expression was significantly increased in *jck* bones compared to WT bones at 8 but not 12 weeks. 1D11 treatment for 1 week completely normalized the increased Sost expression in the 8-week *jck* bones (Fig 11A). To further explore changes in sclerostin, serum Sost levels were measured using a commercially available ELISA assay. However, no significant changes were observed between WT and *jck* mice with or without 1D11 treatment (Fig. 11B).

Discussion

Renal osteodystrophy represents a spectrum of bone diseases from high- to low-turnover In CKD, abnormal bone turnover is associated with dysregulated mineral metabolism,

increased risk for cardiovascular calcification, left ventricular hypertrophy, and mortality. (9,11,46) Identification of additional factors regulating bone turnover, especially in the early stages, is important for understanding the pathogenesis of CKD-MBD. Previously reported longitudinal analysis of *jck* mice demonstrated that the initial stages of high-turnover disease occurred independently of detectable PTH changes. Increased osteoclast activity was likely caused by induction of sclerostin, decreased β-catenin signaling in osteocytes, and a corresponding increase in the RANKL/OPG ratio. (6) Similar changes were found in human bone biopsies suggesting that alterations in Wnt/β-catenin signaling may be a common feature of ROD. This evidence is supported by clinical epidemiologic studies demonstrating increased serum sclerostin in ROD. (28,29)

Jck mice develop CKD as a consequence of activating mutations in Nek8, leading to increased renal expression of polycystin 1 and 2 (PC1 and PC2) with subsequent alterations in cilia structure and function. (24) In contrast, loss of function PKD1 mutations induce polycystic kidney disease and skeletal defects. (26,27) Although primary osteoblast cilia are mechanosensors influencing bone remodeling via β-catenin signaling (47), NEK8 mutations did not influence bone disease – presumably because slight increases in PC1 and PC2 expression do not have the same detrimental effects as no or insufficient levels of these proteins. (6) *In vivo* bone parameters and *ex vivo* bone marrow stromal cell differentiation potential were not different between 6 week old WT and *jck* mice before the onset of renal dysfunction. These observations suggest that observed differences in bone are a consequence of renal dysfunction. Coupled to evidence for similar molecular changes in clinical biopsies, our data supports the use of *jck* mouse as a reasonable model that replicates the salient features of human CKD-MBD with associated high turnover ROD.

Our study focused on TGF-β's potential role on bone in early CKD as this cytokine's positive role in maintaining skeletal health is well known (30,48,49) and TGF-β1 deletion or transgenic inhibition of the TGF-β pathway in osteoblasts results in decreased bone formation. (32,37) Additionally, TGF-β1 circulating levels and bone expression are up-regulated during CKD progression along with increased sclerostin and FGF23. (39,40,50) Elevated TGF-β activity is also associated with enhanced osteoblast and/or osteoclast activity in genetic bone diseases such as Camurati-Engelmann disease (CED) and osteogenesis imperfecta (OI). (31,32,51–54) Finally, TGF-β and Wnt/β-catenin cross-talk has been well described.(34)

The observed elevations of TGF-β1 mRNA, its receptor expression and TGF-β signaling in *jck* mice suggest that TGF-β1 may play an important role in the pathogenesis of high-turnover ROD. TGF-β neutralization in *jck* mice attenuated the elevated levels of bone turnover markers, reduced bone formation rates, decreased osteoclast and osteoblast surface areas, increased trabecular bone volume, and increased cortical thickness with clear reduction in cortical porosity and fibrosis (Fig. 4 and 5). In addition, TGF-β antagonism did not change serum BUN, PTH, Pi or $1,25(OH)_2D_3$ levels suggesting the a direct effect on bone rather than a systemic effect.

Our findings are consistent with the observations of transgenic mice expressing an osteoblast specific truncated type II TGF-β receptor which developed an age-dependent

increase in trabecular bone mass due to decreased resorption and formation. (37) These results coupled to the observations that TGFβ1 expression increases with age raises the possibility that TGFβ1 may contribute to age associated bone loss. In contrast, our findings are distinct from studies in normal juvenile mice, where TGF-β inhibition was associated with increased osteoblast differentiation and decreased osteoclast differentiation. (38,55) Taken together, our results contribute to the growing evidence that TGF-β's effects on bone are dose and context dependent.

The complexity of TGF-β's regulation on bone turnover is illustrated by its influence on osteoblast/osteocyte differentiation, osteoclastogenesis and the coupling between bone formation and resorption. Our findings suggest that blocking TGFβ's actions primarily lead to attenuation of osteoblast activity in the high-turnover ROD setting. We observed increased pSMAD2/SMAD2 expression only in protein extracted from *jck* bone shafts but not bone marrow. It is possible that a small cell sub-population within the bone marrow may also respond to TGF-β as the significant increase in osteoblast precursors derived from *jck* bone marrow is attenuated by TGF-β neutralization (Fig. 10 *A*). Since immunostaining in *jck* bones clearly demonstrated that pSMAD2/3 was induced primarily in osteoblasts and early osteocytes but not osteoclasts (Fig. 2), this observation together with the immunoblot data (Fig. 9) supports a direct role on osteoblast lineage cells. Indeed, the reduced pSMAD2 in osteoblasts and osteocytes was expected as TGF-β's influence on osteoblast lineage is well described both *in vitro* and *in vivo*. TGF-β1 has been shown to temporally influence the differentiation state of osteoblasts through promotion of proliferation and differentiation including increased matrix/osteoid deposition necessary for normal mineralization. Although observed signaling changes were limited to the osteoblast lineage, osteoclast number and activity were significantly suppressed by long-term TGF-β antagonism (Fig. 4, 5 and 7).

As several *in vitro* studies have demonstrated cell and dose dependent effects of TGF-β on osteoclasts via modulation of MAP kinase pathways, we cannot rule out direct effects based on the absence of pSMAD2/3 modulation. (56–60) However, it should be noted that *in vivo* evidence for a direct role of TGF-β on osteoclasts is lacking. Alternatively, TGF-β may modulate osteoclast activity indirectly through the relative ratio of osteoblast/osteocyte expressed RANKL/OPG. Regulation of osteoclast proliferation and/or differentiation by osteoblasts/osteocytes is not a novel mechanism. For example, continuous elevation of PTH leads to increased bone resorption by stimulating RANKL expression in osteoblasts. (61)

TGF-β1 is the key factor responsible for recruitment of osteoblast precursor cells to resorption sites thereby coupling osteoblast and osteoclast differentiation/activity both temporally and spatially. (32,62) Co-staining of TRAP and osterix confirmed increased numbers of remodeling units containing co-localized osteoclasts and osteoblasts with no evidence of resorption/formation de-coupling. Nonetheless, the antibody's effect on bone formation could be at least partially due to the neutralization of osteoclast released TGF-β and subsequent inhibition of osteoblast precursor migration.

All major regulators of bone metabolism contribute to the regulation of osteoblast and osteocyte life span by modulating apoptosis. (63) TGF-β is known to induce apoptosis in a variety of cell types, however data on its role in osteoblastic or osteocytic apoptosis are

contradictory. TGF-β inhibits osteoblast and osteocyte apoptosis *in vitro* (64,65) but mice lacking Smad3 exhibit decreased bone mass associated with increased osteoclast apoptosis. (66) Our data demonstrated that inhibiting TGF-β could attenuate bone disease in CKD with corresponding restoration of Wnt/β-catenin signaling, an important regulator of osteocyte apoptosis. TGF-β could contribute to disease pathogenesis via effects on apoptosis and/or indirectly antagonizing Wnt/β-catenin promotion of survival. However, repression of TGF-β signaling did not have a significant effect on osteocyte apoptosis in *jck* mice as measured by TUNEL staining of bone sections (Fig. 10).

Our whole genome RNA sequencing data from 12 week old mice further validated our previously reported repression of osteocyte Wnt/β-catenin signaling (Table 3 and 4). (6) Wnts (Wnt16, Wnt10b and Wnt5b), Wnt receptors (Frzb and Lrp5), and β-catenin are all significantly suppressed, whereas, negative regulators of Wnts (Sfrp1, Sfrp4 and Dkk1) are significantly elevated. In addition, Pkd1 a known downstream gene for β-catenin is also significantly up-regulated.(26) More importantly, 1 week antagonism of TGF-β normalized expression of β-catenin, casein kinase β2 and Pkd1 expression and modulated other genes associated with stimulation of the Wnt/β-catenin pathway.

Sclerostin is significantly increased in *jck* bones and human biopsies from the early stages of CKD. This change is associated with an expected repression of β-catenin signaling and increased osteoclast activity. (6) Consistent with this finding, our whole genome RNA data from 8 week mice demonstrated that Sost expression was increased 2.3 fold in *jck* bones compared to WT bones ($p < 0.05$). After 1 week of anti-TGF-β administration, Sost expression in the *jck* bones was normalized to levels similar to that in age matched WT mice. ($p < 0.05$ vs. *jck*). At 12 weeks of age, elevated SOST could no longer account for changes in β-catenin signaling, presumably because PTH, a negative regulator of Sost expression is elevated.(67–69) To further confirm our observation, we measured serum Sost levels with an ELISA assay. However, significant changes were not observed between WT and *jck,* or *jck* treated with vehicle or 1D11 at 8 weeks of age. Previously, we demonstrated that mRNA levels as detected by real-time RT-PCR were consistent with changes in sclerostin protein levels as assessed by immunostaining. (6) Taking together, these data raise the possibility that local Sost's effect on bone may predominant. Indeed, *Jastrzebsk,* et al. have recently reported a similar discrepancy between Sost bone mRNA levels and serum protein levels in serum from an ovariectomy model. (70)

The current studies focused solely on initial mechanisms associated with onset of high bone turnover and did not utilize experimental conditions to fully address the potential influence of TGF-β on vascular calcification. Although we have previously demonstrated that *jck* mice do exhibit vascular calcification and early signs of left ventricular hypertrophy, these events occur in significantly older mice than analyzed in the current studies. Similarly, rats treated with high doses of adenine, vitamin D, calcium and phosphorus can also exhibit significant vascular calcification. However, these conditions induce very severe changes in bone disease that do not reflect changes typically observed in clinical biopsies. The adenine model described in our studies exhibits a high-turnover bone disease similar to *jck* mice without the treatments previously described to drive vascular calcification. Additional studies will be required to assess the role of TGF-β on vascular calcification.

In summary, our data demonstrates that increased TGF-β1 expression and signaling is associated with the suppression of Wnt/β-catenin signaling in bone during CKD progression and may contribute to the pathogenesis of high-turnover ROD. TGF-β neutralization attenuates increased bone turnover and improved bone quality via a SMAD dependent restoration of Wnt/β-catenin signaling in osteoblast/osteocytes. Our findings also provide important evidence that TGF-β contributes to the pathogenesis of high-turnover ROD independent of serum PTH level.

Acknowledgments

References

1. Group KC-MW. KDIGO clinical practice guideline for the diagnosis, evaluation, prevention, and treatment of Chronic Kidney Disease-Mineral and Bone Disorder (CKD-MBD). Kidney Int Suppl. 2009; (113):S1–130.

2. Jamal SA, West SL, Miller PD. Fracture risk assessment in patients with chronic kidney disease. Osteoporos Int. 2012; 23(4):1191–8. [PubMed: 21901475]

3. Hamdy NA, Kanis JA, Beneton MN, Brown CB, Juttmann JR, Jordans JG, Josse S, Meyrier A, Lins RL, Fairey IT. Effect of alfacalcidol on natural course of renal bone disease in mild to moderate renal failure. BMJ. 1995; 310(6976):358–63. [PubMed: 7677827]

4. Moe SM, Radcliffe JS, White KE, Gattone VH 2nd, Seifert MF, Chen X, Aldridge B, Chen NX. The pathophysiology of early-stage chronic kidney disease-mineral bone disorder (CKD-MBD) and response to phosphate binders in the rat. J Bone Miner Res. 2011; 26(11):2672–81. [PubMed: 21826734]

5. Wesseling-Perry K, Pereira RC, Tseng CH, Elashoff R, Zaritsky JJ, Yadin O, Sahney S, Gales B, Juppner H, Salusky IB. Early skeletal and biochemical alterations in pediatric chronic kidney disease. Clin J Am Soc Nephrol. 2012; 7(1):146–52. [PubMed: 22052943]

6. Sabbagh Y, Graciolli FG, O'Brien S, Tang W, Dos Reis LM, Ryan S, Phillips L, Boulanger J, Song W, Bracken C, Liu S, Ledbetter S, Dechow P, Canziani ME, Carvalho AB, Jorgetti V, Moyses RM, Schiavi SC. Repression of osteocyte Wnt/beta-catenin signaling is an early event in the progression of renal osteodystrophy. J Bone Miner Res. 2012; 27(8):1757–72. [PubMed: 22492547]

7. Lobao R, Carvalho AB, Cuppari L, Ventura R, Lazaretti-Castro M, Jorgetti V, Vieira JG, Cendoroglo M, Draibe SA. High prevalence of low bone mineral density in pre-dialysis chronic kidney disease patients: bone histomorphometric analysis. Clin Nephrol. 2004; 62(6):432–439. [PubMed: 15630902]

8. Tomiyama C, Carvalho AB, Higa A, Jorgetti V, Draibe SA, Canziani ME. Coronary calcification is associated with lower bone formation rate in CKD patients not yet in dialysis treatment. J Bone Miner Res. 2010; 25 (3):499–504. [PubMed: 19594321]

9. Moe S, Drueke T, Cunningham J, Goodman W, Martin K, Olgaard K, Ott S, Sprague S, Lameire N, Eknoyan G. Kidney Disease: Improving Global O. Definition, evaluation, and classification of renal osteodystrophy: a position statement from Kidney Disease: Improving Global Outcomes (KDIGO). Kidney Int. 2006; 69(11):1945–53. [PubMed: 16641930]

10. Malluche HH, Mawad H, Monier-Faugere MC. The importance of bone health in end-stage renal disease: out of the frying pan, into the fire? Nephrol Dial Transplant. 2004; 19(Suppl 1):i9–13. [PubMed: 15126648]

11. Hruska KA, Mathew S, Lund RJ, Memon I, Saab G. The pathogenesis of vascular calcification in the chronic kidney disease mineral bone disorder: the links between bone and the vasculature. Semin Nephrol. 2009; 29 (2):156–65. [PubMed: 19371806]

12. Price PA, Faus SA, Williamson MK. Bisphosphonates alendronate and ibandronate inhibit artery calcification at doses comparable to those that inhibit bone resorption. Arterioscler Thromb Vasc Biol. 2001; 21 (5):817–24. [PubMed: 11348880]

13. Price PA, June HH, Buckley JR, Williamson MK. Osteoprotegerin inhibits artery calcification induced by warfarin and by vitamin D. Arterioscler Thromb Vasc Biol. 2001; 21(10):1610–6. [PubMed: 11597934]

14. Lomashvili KA, Monier-Faugere MC, Wang X, Malluche HH, O'Neill WC. Effect of bisphosphonates on vascular calcification and bone metabolism in experimental renal failure. Kidney Int. 2009; 75(6):617–25. [PubMed: 19129793]

15. Gonzalez EA, Lund RJ, Martin KJ, McCartney JE, Tondravi MM, Sampath TK, Hruska KA. Treatment of a murine model of high-turnover renal osteodystrophy by exogenous BMP-7. Kidney Int. 2002; 61 (4):1322–31. [PubMed: 11918739]

16. Shanahan CM, Crouthamel MH, Kapustin A, Giachelli CM. Arterial calcification in chronic kidney disease: key roles for calcium and phosphate. Circ Res. 2011; 109(6):697–711. [PubMed: 21885837]

17. Ferreira A, Frazão JM, Monier-Faugere MC, Gil C, Galvao J, Oliveira C, Baldaia J, Rodrigues I, Santos C, Ribeiro S, Hoenger RM, Duggal A, Malluche HH. Sevelamer Study G. Effects of sevelamer hydrochloride and calcium carbonate on renal osteodystrophy in hemodialysis patients. J Am Soc Nephrol. 2008; 19 (2):405–412. [PubMed: 18199805]

18. Mathew S, Lund RJ, Strebeck F, Tustison KS, Geurs T, Hruska KA. Reversal of the adynamic bone disorder and decreased vascular calcification in chronic kidney disease by sevelamer carbonate therapy. J Am Soc Nephrol. 2007; 18(1):122–130. [PubMed: 17182886]

19. Chertow GM, Burke SK, Raggi P. Treat to Goal Working G. Sevelamer attenuates the progression of coronary and aortic calcification in hemodialysis patients. Kidney Int. 2002; 62(1):245–252. [PubMed: 12081584]

20. Drueke TB. Which vitamin D derivative to prescribe for renal patients. Curr Opin Nephrol Hypertens. 2005; 14 (4):343–349. [PubMed: 15931002]

21. Andress DL. Vitamin D in chronic kidney disease: a systemic role for selective vitamin D receptor activation. Kidney Int. 2006; 69(1):33–43. [PubMed: 16374421]

22. Raggi P, James G, Burke SK, Bommer J, Chasan-Taber S, Holzer H, Braun J, Chertow GM. Decrease in thoracic vertebral bone attenuation with calcium-based phosphate binders in hemodialysis. J Bone Miner Res. 2005; 20(5):764–772. [PubMed: 15824849]

23. Stubbs JR, He N, Idiculla A, Gillihan R, Liu S, David V, Hong Y, Quarles LD. Longitudinal evaluation of FGF23 changes and mineral metabolism abnormalities in a mouse model of chronic kidney disease. J Bone Miner Res. 2012; 27(1):38–46. [PubMed: 22031097]

24. Sohara E, Luo Y, Zhang J, Manning DK, Beier DR, Zhou J. Nek8 regulates the expression and localization of polycystin-1 and polycystin-2. J Am Soc Nephrol. 2008; 19(3):469–76. [PubMed: 18235101]

25. Smith LA, Bukanov NO, Husson H, Russo RJ, Barry TC, Taylor AL, Beier DR, Ibraghimov-Beskrovnaya O. Development of polycystic kidney disease in juvenile cystic kidney mice: insights into pathogenesis, ciliary abnormalities, and common features with human disease. J Am Soc Nephrol. 2006; 17(10):2821–31. [PubMed: 16928806]

26. Xiao Z, Zhang S, Cao L, Qiu N, David V, Quarles LD. Conditional disruption of Pkd1 in osteoblasts results in osteopenia due to direct impairment of bone formation. J Biol Chem. 2010; 285(2):1177–87. [PubMed: 19887454]

27. Xiao Z, Zhang S, Mahlios J, Zhou G, Magenheimer BS, Guo D, Dallas SL, Maser R, Calvet JP, Bonewald L, Quarles LD. Cilia-like structures and polycystin-1 in osteoblasts/osteocytes and associated abnormalities in skeletogenesis and Runx2 expression. J Biol Chem. 2006; 281(41): 30884–95. [PubMed: 16905538]

28. Cejka D, Herberth J, Branscum AJ, Fardo DW, Monier-Faugere MC, Diarra D, Haas M, Malluche HH. Sclerostin and Dickkopf-1 in renal osteodystrophy. Clin J Am Soc Nephrol. 2011; 6(4):877–82. [PubMed: 21164019]

29. Pelletier S, Dubourg L, Carlier MC, Hadj-Aissa A, Fouque D. The Relation between Renal Function and Serum Sclerostin in Adult Patients with CKD. Clin J Am Soc Nephrol. 2013

30. Balooch G, Balooch M, Nalla RK, Schilling S, Filvaroff EH, Marshall GW, Marshall SJ, Ritchie RO, Derynck R, Alliston T. TGF-beta regulates the mechanical properties and composition of bone matrix. Proc Natl Acad Sci U S A. 2005; 102(52):18813–8. [PubMed: 16354837]

31. Alliston T. TGF-beta regulation of osteoblast differentiation and bone matrix properties. J Musculoskelet Neuronal Interact. 2006; 6(4):349–50. [PubMed: 17185818]

32. Tang Y, Wu X, Lei W, Pang L, Wan C, Shi Z, Zhao L, Nagy TR, Peng X, Hu J, Feng X, Van Hul W, Wan M, Cao X. TGF-beta1-induced migration of bone mesenchymal stem cells couples bone resorption with formation. Nat Med. 2009; 15(7):757–65. [PubMed: 19584867]

33. Breen EC, Ignotz RA, McCabe L, Stein JL, Stein GS, Lian JB. TGF beta alters growth and differentiation related gene expression in proliferating osteoblasts in vitro, preventing development of the mature bone phenotype. J Cell Physiol. 1994; 160(2):323–35. [PubMed: 8040190]

34. Zhou S. TGF-beta regulates beta-catenin signaling and osteoblast differentiation in human mesenchymal stem cells. J Cell Biochem. 2011; 112(6):1651–60. [PubMed: 21344492]

35. Chen G, Deng C, Li YP. TGF-beta and BMP signaling in osteoblast differentiation and bone formation. Int J Biol Sci. 2012; 8(2):272–88. [PubMed: 22298955]

36. Zhao L, Hantash BM. TGF-beta1 regulates differentiation of bone marrow mesenchymal stem cells. Vitam Horm. 2011; 87:127–41. [PubMed: 22127241]

37. Filvaroff E, Erlebacher A, Ye J, Gitelman SE, Lotz J, Heillman M, Derynck R. Inhibition of TGF-beta receptor signaling in osteoblasts leads to decreased bone remodeling and increased trabecular bone mass. Development. 1999; 126(19):4267–79. [PubMed: 10477295]

38. Edwards JR, Nyman JS, Lwin ST, Moore MM, Esparza J, O'Quinn EC, Hart AJ, Biswas S, Patil CA, Lonning S, Mahadevan-Jansen A, Mundy GR. Inhibition of TGF-beta signaling by 1D11 antibody treatment increases bone mass and quality in vivo. J Bone Miner Res. 2010; 25(11): 2419–26. [PubMed: 20499365]

39. Santos FR, Moyses RM, Montenegro FL, Jorgetti V, Noronha IL. IL-1beta, TNF-alpha, TGF-beta, and bFGF expression in bone biopsies before and after parathyroidectomy. Kidney Int. 2003; 63(3):899–907. [PubMed: 12631070]

40. Duarte ME, Carvalho EF, Cruz EA, Lucena SB, Andress DL. Cytokine accumulation in osteitis fibrosa of renal osteodystrophy. Braz J Med Biol Res. 2002; 35(1):25–9. [PubMed: 11743611]

41. Tamagaki K, Yuan Q, Ohkawa H, Imazeki I, Moriguchi Y, Imai N, Sasaki S, Takeda K, Fukagawa M. Severe hyperparathyroidism with bone abnormalities and metastatic calcification in rats with adenine-induced uraemia. Nephrol Dial Transplant. 2006; 21(3):651–659. [PubMed: 16311258]

42. Parfitt AM, Drezner MK, Glorieux FH, Kanis JA, Malluche H, Meunier PJ, Ott SM, Recker RR. Bone histomorphometry: standardization of nomenclature, symbols, and units. Report of the ASBMR Histomorphometry Nomenclature Committee. J Bone Miner Res. 1987; 2(6):595–610. [PubMed: 3455637]

43. Plotkin LI, Lezcano V, Thostenson J, Weinstein RS, Manolagas SC, Bellido T. Connexin 43 is required for the anti-apoptotic effect of bisphosphonates on osteocytes and osteoblasts in vivo. J Bone Miner Res. 2008; 23(11):1712–21. [PubMed: 18597631]

44. Bivi N, Condon KW, Allen MR, Farlow N, Passeri G, Brun LR, Rhee Y, Bellido T, Plotkin LI. Cell autonomous requirement of connexin 43 for osteocyte survival: consequences for endocortical resorption and periosteal bone formation. J Bone Miner Res. 2012; 27(2):374–89. [PubMed: 22028311]

45. Bouxsein ML, Boyd SK, Christiansen BA, Guldberg RE, Jepsen KJ, Muller R. Guidelines for assessment of bone microstructure in rodents using micro-computed tomography. J Bone Miner Res. 2010; 25 (7):1468–86. [PubMed: 20533309]

46. London GM, Marty C, Marchais SJ, Guerin AP, Metivier F, de Vernejoul MC. Arterial calcifications and bone histomorphometry in end-stage renal disease. J Am Soc Nephrol. 2004; 15(7):1943–51. [PubMed: 15213285]

47. Wallingford JB, Mitchell B. Strange as it may seem: the many links between Wnt signalling, planar cell polarity, and cilia. Genes and Development. 2011; 25:201–213. [PubMed: 21289065]

48. Mundy GR, Bonewald LF. Role of TGF beta in bone remodeling. Ann N Y Acad Sci. 1990; 593:91–7. [PubMed: 2197964]

49. Janssens K, ten Dijke P, Janssens S, Van Hul W. Transforming growth factor-beta1 to the bone. Endocr Rev. 2005; 26(6):743–74. [PubMed: 15901668]

50. Lee SB, Kanasaki K, Kalluri R. Circulating TGF-beta1 as a reliable biomarker for chronic kidney disease progression in the African-American population. Kidney Int. 2009; 76(1):10–2. [PubMed: 19528989]

51. Kinoshita A, Saito T, Tomita H, Makita Y, Yoshida K, Ghadami M, Yamada K, Kondo S, Ikegawa S, Nishimura G, Fukushima Y, Nakagomi T, Saito H, Sugimoto T, Kamegaya M, Hisa K, Murray JC, Taniguchi N, Niikawa N, Yoshiura K. Domain-specific mutations in TGFB1 result in Camurati-Engelmann disease. Nat Genet. 2000; 26(1):19–20. [PubMed: 10973241]

52. Hernandez MV, Peris P, Guanabens N, Alvarez L, Monegal A, Pons F, Ponce A, Munoz-Gomez J. Biochemical markers of bone turnover in Camurati-Engelmann disease: a report on four cases in one family. Calcif Tissue Int. 1997; 61(1):48–51. [PubMed: 9192513]

53. Whyte MP, Totty WG, Novack DV, Zhang X, Wenkert D, Mumm S. Camurati-Engelmann disease: unique variant featuring a novel mutation in TGFbeta1 encoding transforming growth factor beta 1 and a missense change in TNFSF11 encoding RANK ligand. J Bone Miner Res. 2011; 26(5):920–33. [PubMed: 21541994]

54. Gebken J, Brenner R, Feydt A, Notbohm H, Brinckmann J, Muller PK, Batge B. Increased cell surface expression of receptors for transforming growth factor-beta on osteoblasts from patients with Osteogenesis imperfecta. Pathobiology. 2000; 68(3):106–12. [PubMed: 11174067]

55. Mohammad KS, Chen CG, Balooch G, Stebbins E, McKenna CR, Davis H, Niewolna M, Peng XH, Nguyen DH, Ionova-Martin SS, Bracey JW, Hogue WR, Wong DH, Ritchie RO, Suva LJ, Derynck R, Guise TA, Alliston T. Pharmacologic inhibition of the TGF-beta type I receptor kinase has anabolic and anti-catabolic effects on bone. PLoS One. 2009; 4(4):e5275. [PubMed: 19357790]

56. Cicek M, Vrabel A, Sturchio C, Pederson L, Hawse JR, Subramaniam M, Spelsberg TC, Oursler MJ. TGF-beta inducible early gene 1 regulates osteoclast differentiation and survival by mediating the NFATc1, AKT, and MEK/ERK signaling pathways. PLoS One. 2011; 6(3):e17522. [PubMed: 21423731]

57. Houde N, Chamoux E, Bisson M, Roux S. Transforming growth factor-beta1 (TGF-beta1) induces human osteoclast apoptosis by up-regulating Bim. J Biol Chem. 2009; 284(35):23397–404. [PubMed: 19574221]

58. Gingery A, Bradley EW, Pederson L, Ruan M, Horwood NJ, Oursler MJ. TGF-beta coordinately activates TAK1/MEK/AKT/NFkB and SMAD pathways to promote osteoclast survival. Exp Cell Res. 2008; 314(15):2725–38. [PubMed: 18586026]

59. Karst M, Gorny G, Galvin RJ, Oursler MJ. Roles of stromal cell RANKL, OPG, and M-CSF expression in biphasic TGF-beta regulation of osteoclast differentiation. J Cell Physiol. 2004; 200(1):99–106. [PubMed: 15137062]

60. Yasui T, Kadono Y, Nakamura M, Oshima Y, Matsumoto T, Masuda H, Hirose J, Omata Y, Yasuda H, Imamura T, Nakamura K, Tanaka S. Regulation of RANKL-induced osteoclastogenesis by TGF-beta through molecular interaction between Smad3 and Traf6. J Bone Miner Res. 2011; 26(7):1447–56. [PubMed: 21305609]

61. Silva BC, Costa AG, Cusano NE, Kousteni S, Bilezikian JP. Catabolic and anabolic actions of parathyroid hormone on the skeleton. J Endocrinol Invest. 2011; 34(10):801–10. [PubMed: 21946081]

62. Mundy GR. The effects of TGF-beta on bone. Ciba Found Symp. 1991; 157:137–43. discussion 143–51. [PubMed: 2070682]

63. Jilka RL, Weinstein RS, Parfitt AM, Manolagas SC. Quantifying osteoblast and osteocyte apoptosis: challenges and rewards. J Bone Miner Res. 2007; 22(10):1492–501. [PubMed: 17542686]

64. Jilka RL, Weinstein RS, Bellido T, Parfitt AM, Manolagas SC. Osteoblast programmed cell death (apoptosis): modulation by growth factors and cytokines. J Bone Miner Res. 1998; 13(5):793–802. [PubMed: 9610743]

65. Bodine PV, Billiard J, Moran RA, Ponce-de-Leon H, McLarney S, Mangine A, Scrimo MJ, Bhat RA, Stauffer B, Green J, Stein GS, Lian JB, Komm BS. The Wnt antagonist secreted frizzled-

related protein-1 controls osteoblast and osteocyte apoptosis. J Cell Biochem. 2005; 96(6):1212–30. [PubMed: 16149051]

66. Borton AJ, Frederick JP, Datto MB, Wang XF, Weinstein RS. The loss of Smad3 results in a lower rate of bone formation and osteopenia through dysregulation of osteoblast differentiation and apoptosis. J Bone Miner Res. 2001; 16(10):1754–64. [PubMed: 11585338]

67. Keller H, Kneissel M. SOST is a target gene for PTH in bone. Bone. 2005; 37(2):148–58. [PubMed: 15946907]

68. Silvestrini G, Ballanti P, Leopizzi M, Sebastiani M, Berni S, Di Vito M, Bonucci E. Effects of intermittent parathyroid hormone (PTH) administration on SOST mRNA and protein in rat bone. J Mol Histol. 2007; 38(4):261–9. [PubMed: 17549589]

69. Trombetti A, Cortes F, Kaelin A, Morris M, Rizzoli R. Intranasal calcitonin reducing bone pain in a patient with Camurati-Engelmann disease. Scand J Rheumatol. 2012; 41(1):75–7. [PubMed: 22044122]

70. Jastrzebski S, Kalinowski J, Stolina M, Mirza F, Torreggiani E, Kalajzic I, Won HY, Lee SK, Lorenzo J. Changes in bone sclerostin levels in mice after ovariectomy vary independently of changes in serum sclerostin levels. J Bone Miner Res. 2013; 28(3):618–26. [PubMed: 23044658]
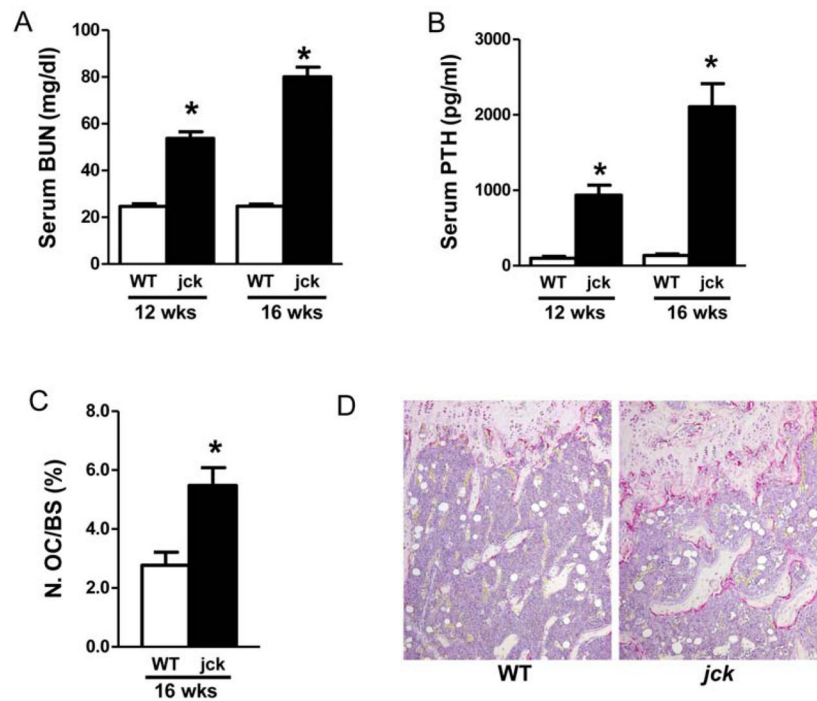
Fig. 1.

Jck mice develop high-turnover bone disease during progression of chronic kidney disease. (*A*) Serum BUN levels, a marker of kidney function are elevated progressively in *jck* mice whereas no change is observed in WT mice. (*B*) Serum PTH levels are significantly elevated at 12 weeks and further increased at week 16. (*C*) Number of osteoclasts is significantly increased in *jck* mice. (*D*) Representative TRAP staining shows significant increases in N. OC/BS (%) at 16 weeks of age. (10 X objective lens). Results are expressed as mean ± SEM. * indicates $p < 0.05$ compared with age-matched WT mice by t-test (n   10)
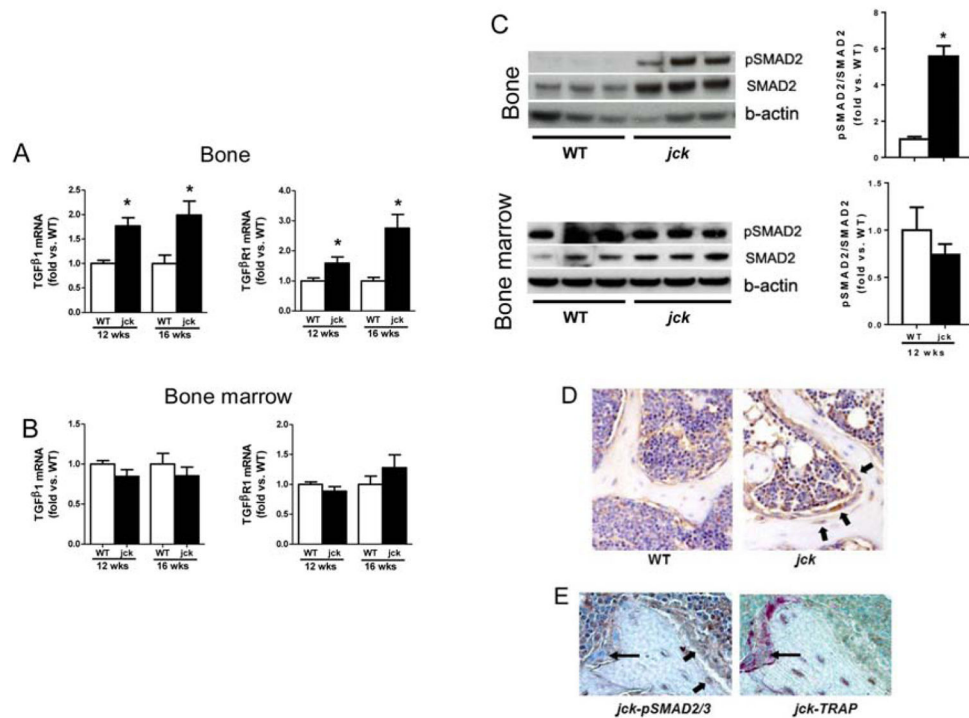
Fig. 2.
TGF-β1 and TGF-β signaling in bone and bone marrow of *jck* mice. Quantitative RT-PCR measurement shows (*A*) TGF-β1 and TGFβR1 gene expression are increased in bones of *jck* compared with WT mice by 12 weeks of ages (n = 6). (*B*) TGF-β1 and TGFβR1 gene expression are not altered in bone marrow of *jck* mice (n = 6). (*C*) Western blot analysis and quantitative measurement of the fold changes shows pSMAD2, a downstream signal of TGF-β action is increased in bone but not in bone marrow of *jck* mice at 12 weeks of age (n = 3). Values in Fig A, B and C are expressed as mean ± SEM. * indicates p < 0.05 compared with age-matched WT mice by *t*-test. (*D*) Immunostaining with anti-pSMAD2/3 on decalcified femur sections shows that pSMAD2/3 is increased in osteoblasts and early osteocytes in *jck* mice (black arrow) (n = 6 in WT group and n = 8 in *jck* group). (E) Immunostaining and TRAP staining on serial femur sections shows pSMAD2/3 are expressed in osteoblasts (TRAP negative, wide arrows) but not expressed in osteoclasts (n = 6 in WT group and n = 8 in *jck* group).
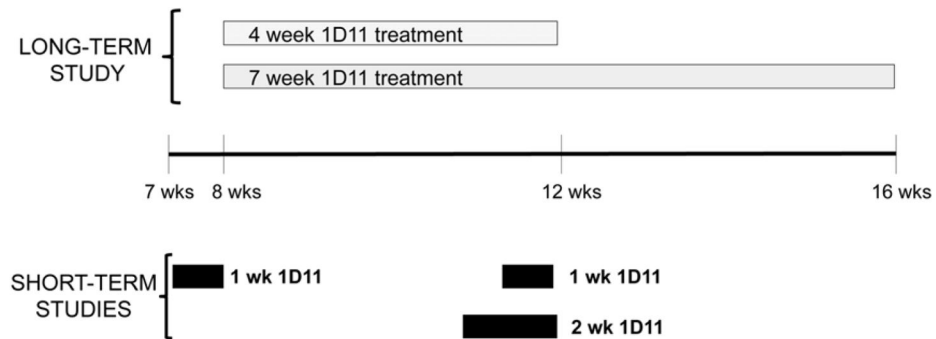
Fig. 3.
Study designs to assess 1D11 long-term effect and short-term effect on bone in *jck* mice. To evaluate the long term effect of 1D11 on bone, 1D11 or vehicle was given to *jck* mice at 8 weeks of age via intraperitoneal injection 3 times per week at 2 or 5 mg/kg. Blood and tissues were harvested after 4 or 7 weeks of treatment. To examine the effect of 1D11 on osteoblast or osteoclast precursors in bone marrow *jck* mice were treated with PBS or 1D11 for 2 weeks, and bone marrow was harvested for MSC and HSC culture. To examine the effect of 1D11 on gene expression, 7 or 11 week old *jck* mice were injected IP with PBS or 1D11 at 5mg/kg on day 1, 3, 5 and 7, and sacrificed on day 8. Bone shafts of tibias and femurs were harvested for RNA or protein expression analysis.
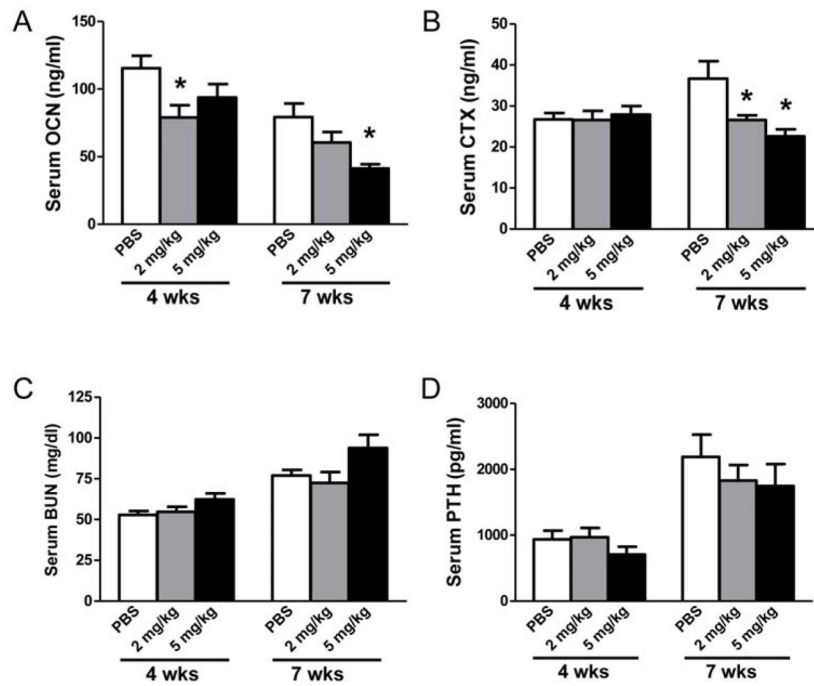
Fig. 4.
1D11 significantly suppresses bone turnover markers in *jck* mice. (*A*) Serum osteocalcin (OCN) and (*B*) C-terminal cross-linking telopeptide of type I collagen (CTX) levels were suppressed significantly in *jck* mice after 7 weeks of treatment. (*C*) Serum BUN, and (*D*) PTH levels were not affected by 1D11 treatment. Results are expressed as mean ± SEM. * indicates p < 0.05 compared with age-matched *jck* mice treated with PBS by one-way ANOVA and Tukey's multiple comparison test (n   12 in the 4 week treatment groups; n 8 in the 7 week treatment groups).
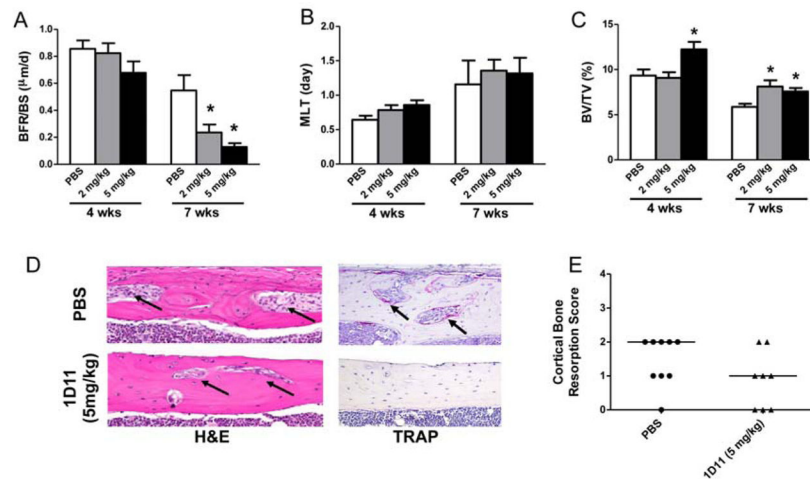
Fig. 5.
Effect of 1D11 on TMV classification (turnover, mineralization and volume) and cortical bone resorption. 8 week old *jck* mice were treated with 1D11 as described in the "Methods" and Fig 3. (*A*) 1D11 dose-dependently suppresses bone formation rate (BFR/BS) after 7 weeks of treatment. (*B*) 1D11 has no impact on bone mineralization measured by mineralization lag time (MLT). (*C*) 1D11 increases BV/TV (%) after 4 weeks at 5 mg/kg dose and after 7 week treatment at both 2 and 5 mg/kg doses. Results are expressed as mean ± SEM. * indicates $p < 0.05$ compared with age-matched *jck* mice treated with PBS by one-way ANOVA and Tukey's multiple comparison test (n 12 in the 4 week treatment groups; n 8 in the 7 week treatment groups). (*D*) Representative H&E and TRAP stained sections from femurs showing 1D11 reduces cortical bone resorption (porosity, black arrow). (*E*) semi-quantitative scores of cortical bone resorption shows a trend toward decreased cortical porosity.
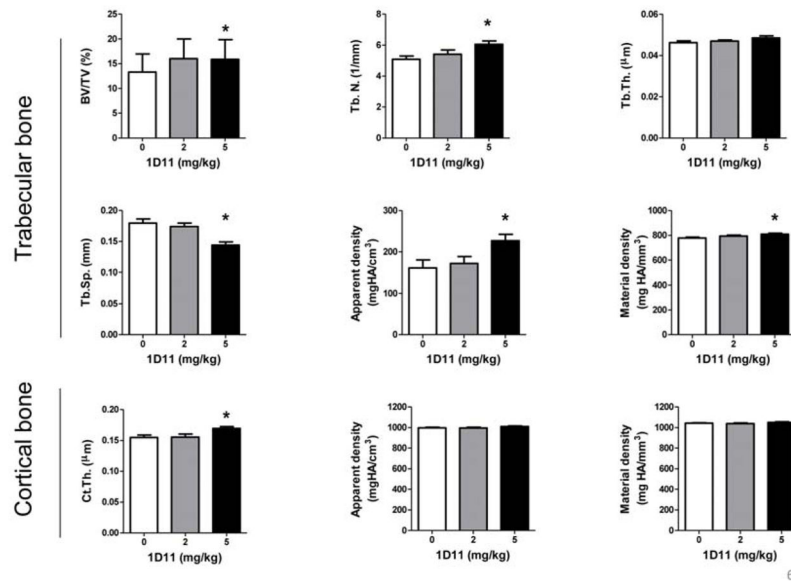
Fig. 6.
MicroCT measurement shows improvement of bone quality in both trabecular and cortical bone after 4 week treatment with 1D11. 1D11 treatment at 5 mg/kg significantly increases BV/TV, Tb. N. but not Tb.Th. 1D11 treatment suppresses Tb.Sp. and increases apparent density and material density. 1D11 also increases Ct.Th. Data are shown as mean ± SEM. * indicates $p < 0.05$ versus PBS treated *jck* mice by one-way ANOVA and Tukey's multiple comparison test (n = 14). BV/TV, bone volume/tissue volume; Tb.Th, trabecular thickness; Tb.N, trabecular number; Tb.Sp, trabecular separation; Ct.Th, cortical thickness.
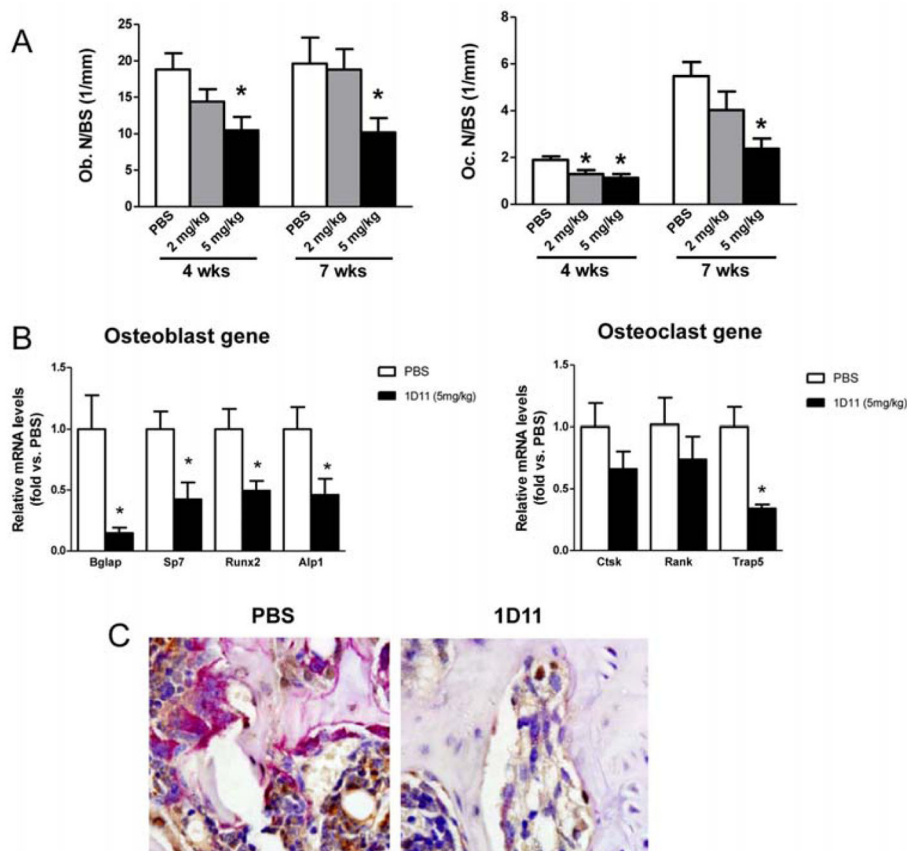
Fig. 7.
1D11 treatment suppresses both osteoblast and osteoclast numbers. (*A*) Bone histomorphometric analysis shows 1D11 significantly suppresses Ob.N and Oc.N on bone surface (n   7). (*B*) Quantitative RT-PCR measurement shows suppressed mRNA expression of osteoblast and osteoclast markers in bone from *jck* mice treated with 1D11 vs. untreated mice (n = 6). Bglap, bone gamma-carboxyglutamate protein (osteocalcin); Sp7, transcription factor 7 (oserix); Runx2, runt related transcription factor 2; Alpl, alkaline phosphatase; Ctsk, cathepsin K; Rank, receptor activator of NF-KB; Trap5, tartrate-resistant acid phosphatase type 5. (*C*) Co-staining of TRAP and anti-osterix antibody staining on sections from decalcified femur shows decreased TRAP positive osteoclasts (pink) and osterix positive osteoblast precursors (brown) in femur from mice treated with 1D11 vs. untreated for 7 weeks. Data are shown as mean ± SEM. * indicates p < 0.05 versus PBS treated *jck* mice by one-way ANOVA and Tukey's multiple comparison (A) or t-test (B).
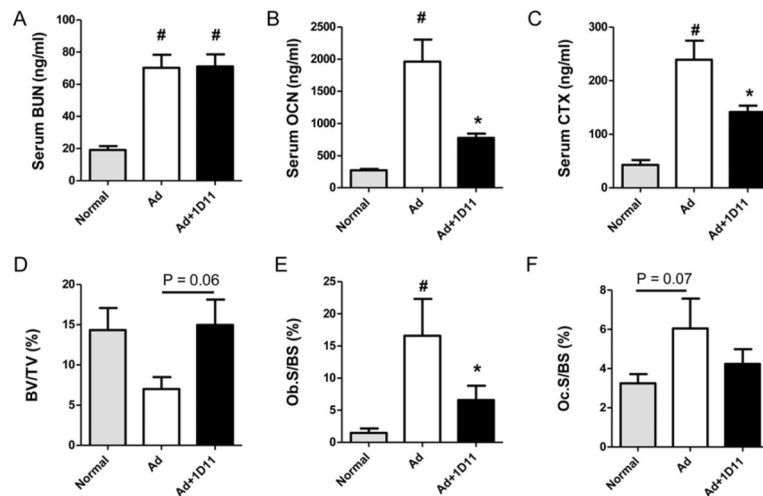
Fig. 8.
Bone turnover is increased in an adenine (Ad)-induced rat CKD model and 1D11 attenuates the elevation in bone turnover. Standard rodent diet mixed with 0.3 and 0.6% adenine was used to induce kidney damage in rat and evaluate 1D11's effect on bone as described in the "Methods". (A) Adenine induces kidney function damage as measured by increased serum BUN levels; 1D11 has no effect on serum BUN levels. (B, C). Serum bone turnover makers, OCN and CTX are significantly elevated in rats treated with adenine. 1D11 attenuates the elevation of serum OCN and CTX. (D–F). Bone histomorphometric analysis shows a trend toward decreased fractional bone volume (BV/TV) and increased osteoblast surface (Ob. S/BS) and osteoclast surface (Oc. S/BS) in adenine induced CKD. 1D11 treatment significantly attenuates the increase in Ob.S/BS and is associated with a trend toward increased BV/TV (p =0.06) and decreased Oc.S/BS (p = 0.07). Data are shown as mean ± SEM. # indicates $p < 0.05$ compared with normal controls and * indicates $p < 0.05$ compared with PBS-treated adenine induced CKD rats (Ad) by one-way ANOVA and Tukey's multiple comparison test (n = 8 per group).
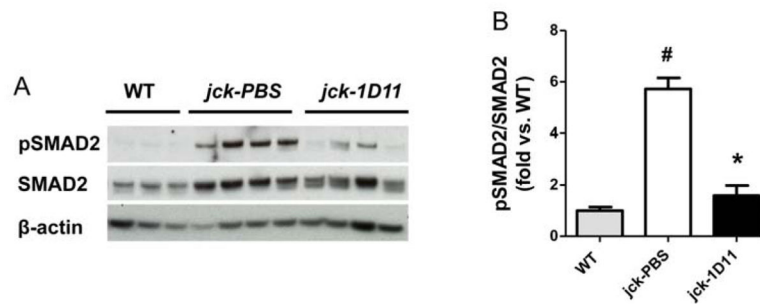
Fig. 9.
1D11 suppresses SMAD2 phosphorylation in *jck* bone. Eleven week old *jck* mice received 4 doses of 1D11 (5 mg/kg) prior to sacrifice (see details in Methods and Fig. 3). (*A*) Immunobloting of protein extracted from mid-shaft of femurs of WT and *jck* mice shows pSMAD2 expression is significantly increased in *jck* bone and is attenuated by 1D11 treatment. (B) Quantitative measurement of the fold changes of pSMAD2/SMAD2 of immunoblotting in panel (A) indicates that there is a significant increase in the pSMAD2/SMAD2 ratio in *jck* mice relative to WT that was significantly suppressed by 1D11 treatment. Data are shown as mean ± SEM. # indicates $p < 0.05$ compared with WT mice and * indicates $p < 0.05$ compared with PBS-treated *jck* mice by one-way ANOVA and Tukey's multiple comparison test. Data from WT and *jck* mice were from the same experiment as described in Fig 2 *C*.
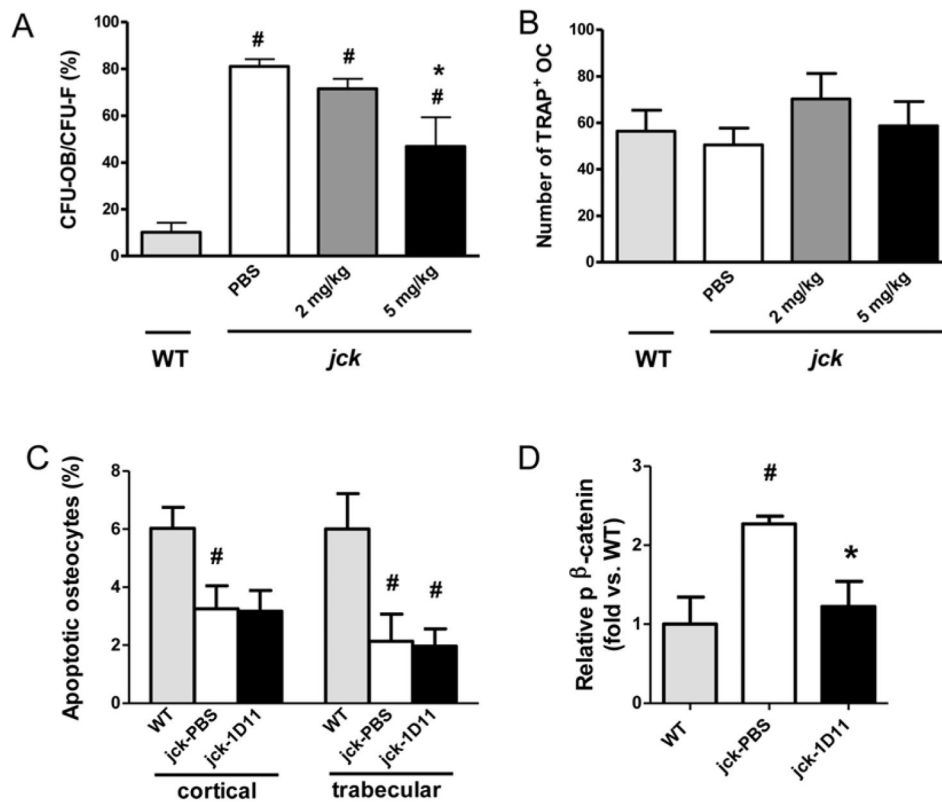
Fig. 10.

Effects of 1D11 on proliferation and differentiation of osteoblast precursors and osteoclastogenesis in bone marrow, apoptosis of osteocytes, and p-β-catenin in bone of *jck* mice. *Jck* mice at 10 weeks of age were treated with PBS, 2 or 5 mg/kg 1D11 for two weeks. (*A*) Bone marrow cells were isolated and cultured in the condition favoring osteoblast differentiation (n = 5). CFU-OB/CFU-F ratios are significantly elevated in MSC from *jck* mice treated with PBS vs WT mice and 1D11 at 5 mg/kg significantly attenuated the elevation of CFU-OB/CFU-F in *jck* mice. (*B*) Bone marrow cells were cultured in media favoring differentiation to osteoclastogenesis (n = 5). Number of TRAP+ osteoclasts in *jck* mice are not different from WT mice and 1D11 treatment has no effect on osteoclastogenesis. *(C)* Apoptosis of osteocytes from WT mice and *jck* mice treated with PBS or 1D11 (5 mg/kg) for 4 weeks were measured by TUNEL staining (n= 7 in WT group and 10 in *jck* group). The percentage of apoptotic osteocytes was significantly decreased in both cortical and trabecular bone of *jck* compared to age-matched WT mice. 1D11 (5 mg/kg) treatment had no significant effect on the number of apoptotic osteocytes in *jck* mice. (*D*) 1D11 suppressed the increased p-β-catenin in bone. Eleven week old *jck* mice received 4 doses of 1D11 (5 mg/kg) prior to sacrifice (see details in Methods and Fig. 3). Immunoblotting of protein extracted from mid-shaft of femurs of WT and *jck* mice shows p-β-catenin expression is significantly increased in *jck* bone and attenuated by 1D11 treatment (n = 4). Data are shown as mean ± SEM. # indicates $p < 0.05$ compared with WT mice and * indicates $p < 0.05$ compared with *jck* mice treated with PBS by one-way ANOVA and Tukey's multiple comparison test.
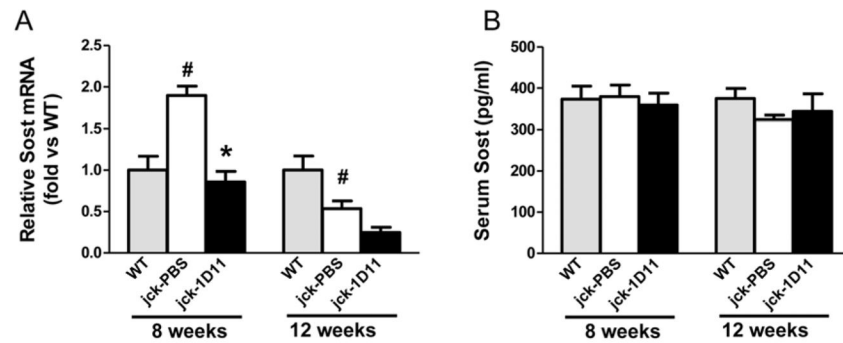
Fig. 11.
Effect of 1D11 on Sost expression in bone. 7- and 11-week old *jck* mice treated with PBS or 1D11 (5 mg/kg) at days 1, 3, 5 and 7. Long bones were collected from these animals and age-matched WT mice to serve as controls at day 8 (8 or 12 weeks old). (*A*) Total RNA was extracted from tibia and femur bone shafts and whole genome mRNA expression were analyzed. Sost mRNA levels were significantly elevated in *jck* bones at 8 weeks but suppressed at 12 week. 1D11 treatment suppressed Sost expression in *jck* bone at both 8 and 12 weeks. (*B*) serum Sost levels were not different between WT and *jck* mice and 1D11 treatment had no effect on serum Sost levels. Data are shown as mean ± SEM. # indicates p < 0.05 compared with WT mice and * indicates p < 0.05 compared with *jck* mice treated with PBS by one-way ANOVA and Tukey's multiple comparison test (n = 6).

Table 1

Serum biochemistry values of *jck* mice after 4 and 7 weeks of treatment

	4 week treatment			7 week treatment		
	PBS	1D11 (2 mg/kg)	1D11 (5 mg/kg)	PBS	1D11 (2 mg/kg)	1D11 (5 mg/kg)
BUN (mg/dl)	53 ± 2	55 ± 3	62 ± 4	77 ± 3	72 ± 7	93 ± 8
Creatinine (mg/dl)	0.26 ± 0.02	0.27 ± 0.02	0.24 ± 0.01	0.27 ± 0.07	0.26 ± 0.05	0.29 ± 0.02
Phosphate (mg/dl)	11.1 ± 0.6	10.1 ± 0.6	$8.8 \pm 0.4^*$	11.2 ± 0.7	9.8 ± 0.7	11.1 ± 0.9
Calcium (mg/dl)	8.7 ± 0.2	8.6 ± 0.2	8.9 ± 0.2	7.1 ± 0.2	7.6 ± 0.1	6.8 ± 0.2
FGF23 (pg/ml)	27967 ± 7442	39979 ± 11067	15706 ± 2777	8818 ± 2413	9369 ± 2705	9813 ± 2104
PTH (pg/ml)	935 ± 132	968 ± 143	707 ± 119	2190 ± 335	1828 ± 240	1745 ± 334
1,25-$(OH)_2$D (pg/ml)	239 ± 13	242 ± 12	233 ± 14	365 ± 38	448 ± 37	351 ± 37
Osteocalcin (ng/ml)	115 ± 9	$72 \pm 6^*$	94 ± 10	79 ± 10	$60 \pm 8^*$	$41 \pm 3^*$
CTX (ng/ml)	27 ± 2	27 ± 2	28 ± 2	37 ± 4	27 ± 1	$23 \pm 2^*$
P1NP (ng/ml)	ND	ND	ND	30 ± 6	23 ± 4	$11 \pm 2^*$

Data are shown as mean ± SEM.

*
indicates p < 0.05 versus PBS treated age-matched jck mice by one-way ANOVA and Tukey's multiple comparison test (n ≥ 12 in the 4 week treatment groups; n ≥ 8 in the 7 week treatment groups).

ND, not determined.

Table 2

Bone histomorphometric analysis of *jck* bones

	4 week treatment			7 week treatment		
	PBS	1D11 (2mg/kg)	1D11 (5mg/kg)	PBS	1D11 (2mg/kg)	1D11 (5mg/kg)
TV/BV (%)	9.3±0.7	9.1±0.6	12.2±0.8*	5.9±0.4	8.1±0.6*	7.6±0.4*
Tb.Th. (mm)	0.065±0.002	0.065±0.002	0.072±0.002*	0.058±0.003	0.068±0.004	0.065±0.004
Tb.N.(1/mm²)	5.2±0.1	5.3±0.1	5.5±0.1	4.9±0.1	5.1±0.1	5.2±0.1
Tb.Sp (mm)	0.13±0.003	0.13±0.003	0.11±0.003	0.15±0.004	0.13±0.004	0.13±0.004
MS/BS (%)	0.24±0.19	0.23±0.04	0.20±0.02	0.25±0.04	0.18±0.02	0.14±0.27
MAR (mm/day)	3.18±0.17	2.70±0.24	2.56±0.25	1.65±0.28	1.16±0.17	0.90±0.05
BFR/BS (mm³/mm²/yr)	0.77±0.08	0.76±0.08	0.54±0.08	0.55±0.11	0.24±0.06	0.13±0.29
MLT (day)	1.16±0.35	1.36 ± 0.16	1.32 ± 0.23	0.64±0.06	0.79±0.07	0.86±0.07
OV/BV (%)	0.017±0.004	0.012±0.003	0.010±0.003	0.66 ± 0.38	0.58±0.38	0.001±0.00
N. Ob./BS (%)	18.8±2.2	14.4±1.7	10.5±1.8*	19.6±3.6	18.8±2.8	10.2±2.0*
N.Oc./BS(%)	1.9±0.15	1.3±0.16*	1.1±0.17*	5.5±0.61	4.0±0.79	2.4±0.45*

Data are shown as mean ± SEM from histomorphometric analysis.

*
 indicates p < 0.05 versus PBS treated age-matched *jck* mice by one-way ANOVA and Tukey's multiple comparison test (n   12 in the 4 week treatment groups; n   7 in the 7 week treatment groups).

BV/TV, bone volume/tissue volume; Tb.Th, trabecular thickness; Tb.N, trabecular number; Tb.Sp, trabecular separation; MS/BS, mineralizing surface/bone surface; MAR, mineral apposition rate; BFR/BS, bone formation rate/bone surface; MLT, mineralization lag time; OV/BV osteoid volume/bone volume; N.Ob./BS, number of osteoblasts/bone surface; N.Oc./BS, number of osteoclasts/bone surface;

Table 3

Genes with significant expression change in *jck* bone compared with WT bones (1.3 fold and p < 0.05, n = 6) at 12 weeks of age

Gene	Description	*jck* vs WT (fold)
Frzb	frizzled-related protein	−3.54
Wnt16	wingless-type MMTV integration site family, member 16	−2.35
Dkk3	dickkopf 3 homolog (Xenopus laevis)	−2.16
Sost	sclerostin	−2.00
Tgfb3	transforming growth factor, beta 3	−1.90
Wnt10b	wingless-type MMTV integration site family, member 10B	−1.80
Wnt5b	wingless-type MMTV integration site family, member 5B	−1.77
Cdh2	cadherin 2, type 1, N-cadherin (neuronal)	−1.57
Wif1	WNT inhibitory factor 1	−1.55
Sox17	SRY (sex determining region Y)-box 17	−1.38
Ctnnb1	catenin (cadherin-associated protein), beta 1, 88kDa	−1.38
Kremen1	kringle containing transmembrane protein 1	−1.37
Ppp2r5b	protein phosphatase 2, regulatory subunit B′, beta	−1.37
Lrp5	low density lipoprotein receptor-related protein 5	−1.36
Smo	smoothened, frizzled family receptor	−1.34
Sfrp1	secreted frizzled-related protein 1	2.06
Sfrp4	secreted frizzled-related protein 4	1.80
Dkkl1	dickkopf-like 1	1.80
Crebbp	CREB binding protein	1.51
Map4k1	mitogen-activated protein kinase kinase kinase kinase 1	1.48
Tgfbr1	transforming growth factor, beta receptor 1	1.43
Pkd1	polycystic kidney disease 1	1.40
Csnk2b	casein kinase 2, beta polypeptide	1.39
Rara	retinoic acid receptor, alpha	1.36
Cd44	CD44 molecule (Indian blood group)	1.33
Csnk1g1	casein kinase 1, gamma 1	1.32
Sox12	SRY (sex determining region Y)-box 12	1.31
Tgfb1	transforming growth factor, beta 1	1.30
Ep300	E1A binding protein p300	1.30

Table 4

Genes with significant expression change (> 1.2 fold, p < 0.05, n = 6) in bones from 1D11 treated *jck* mice compared with PBS-treated ones at 12 weeks of age

Gene	Description	1D11 vs PBS (fold)	*jck* vs WT (fold)
Csnk2b	casein kinase 2, beta polypeptide	−1.29	1.39
Dvl3	dishevelled, dsh homolog 3 (Drosophila)	1.56	N.S.
Pkd1	polycystic kidney disease 1	1.41	−1.40
Smo	smoothened, frizzled family receptor	1.34	−1.34
Ctnnb1	catenin (cadherin-associated protein), beta 1, 88kDa	1.31	−1.36
Appl2	adaptor protein, phosphotyrosine interaction, PH domain and leucine zipper containing 2	1.31	N.S.
Fzd5	frizzled family receptor 5	1.26	N.S.
Dvl1	dishevelled, dsh homolog 1 (Drosophila)	1.20	−1.16

N.S, not significant